Title

Iron-regulatory genes are associated with Neuroimaging measures in HIV infection.

Authors

Fennema-Notestine, Christine
Thornton-Wells, Tricia A
Hulgan, Todd
et al.

Publication Date

2019-07-03

DOI

10.1007/s11682-019-00153-0

Peer reviewed

Brain Imaging and Behavior
https://doi.org/10.1007/s11682-019-00153-0

ORIGINAL RESEARCH

Iron-regulatory genes are associated with Neuroimaging measures in HIV infection

Christine Fennema-Notestine[1,2] · Tricia A. Thornton-Wells[3] · Todd Hulgan[4] · Scott Letendre[5] · Ronald J. Ellis[1,6] · Donald R. Franklin Jr[1] · Albert M. Anderson[7] · Robert K. Heaton[1] · Cinnamon S. Bloss[1,8] · Igor Grant[1] · Asha R. Kallianpur[9,10] · for the CHARTER Study Group

Abstract

The pathogenesis of HIV-associated neurocognitive impairment (NCI) may involve iron dysregulation. In 243 HIV-seropositive adults without severe comorbidities, we therefore genotyped 250 variants in 20 iron-related genes and evaluated their associations with magnetic resonance imaging measures of brain structure and metabolites, including measures previously linked to NCI. Multivariable regression analyses examined associations between genetic variants and neuroimaging measures, adjusting for relevant covariates and multiple testing. Exploratory analyses stratified by NCI (Global Deficit Score ≥ 0.5 vs. <0.5), virus detectability in plasma, and comorbidity levels were also performed. Of 27 variants (in 12 iron-regulatory genes) associated with neuroimaging measures after correction for the 37 haplotype blocks represented, 3 variants survived additional correction for the 21 neuroimaging measures evaluated and demonstrated biologically plausible associations. *SLC11A1* rs7576974_*T* was significantly associated with higher frontal gray matter *N*-acetylaspartate ($p = 3.62e^{-5}$). Among individuals with detectable plasma virus, *TFRC* rs17091382_*A* was associated with smaller subcortical gray matter volume ($p = 3.23e^{-5}$), and *CP* rs4974389_*A* ($p = 3.52e^{-5}$) was associated with higher basal ganglia Choline in persons with mild comorbidities. Two other strong associations were observed for variants in *SLC40A1* and *ACO2* but were not robust due to low minor-allele frequencies in the study sample. Variants in iron metabolism and transport genes are associated with structural and metabolite neuroimaging measures in HIV-seropositive adults, regardless of virus suppression on antiretroviral therapy. These variants may confer susceptibility to HIV-related brain injury and NCI. Further studies are needed to determine the specificity of these findings to HIV infection and explore potential underlying mechanisms.

Keywords Iron-regulatory gene · Brain · Structural MRI · Magnetic resonance spectroscopy (MRS) · HIV · Association studies in genetics

Electronic supplementary material The online version of this article (https://doi.org/10.1007/s11682-019-00153-0) contains supplementary material, which is available to authorized users.

✉ Christine Fennema-Notestine
fennema@ucsd.edu

[1] Department of Psychiatry, University of California-San Diego, 9500 Gilman Dr., #0738, La Jolla, CA 92093-0738, USA

[2] Department of Radiology, University of California-San Diego, La Jolla, CA, USA

[3] Department of Molecular Physiology & Biophysics and Department of Biomedical Informatics, Vanderbilt University School of Medicine, Nashville, TN, USA

[4] Department of Medicine, Division of Infectious Diseases, Vanderbilt University Medical Center, Nashville, TN, USA

[5] Department of Medicine, Division of Infectious Diseases, University of California-San Diego, La Jolla, CA, USA

[6] Department of Neurosciences, University of California-San Diego, La Jolla, CA, USA

[7] Department of Medicine, Emory University School of Medicine, Atlanta, GA, USA

[8] Department of Family Medicine and Public Health, University of California-San Diego, La Jolla, CA, USA

[9] Department of Genomic Medicine, Lerner Research Institute, Cleveland Clinic, Cleveland, OH, USA

[10] Department of Molecular Medicine, Cleveland Clinic Lerner College of Medicine of Case Western Reserve University, Cleveland, OH, USA

Published online: 03 July 2019

Introduction

Despite effective antiretroviral therapy (ART), HIV-associated neurocognitive impairment (NCI) remains common in HIV-seropositive (HIV+) individuals and is rising in prevalence (Heaton et al. 2015; Sheppard et al. 2015). Recent studies suggest that brain alterations occur even during successful ART and at early stages of infection and are associated with NCI (Harezlak et al. 2011; Cysique et al. 2018; Fennema-Notestine et al. 2013; Valcour et al. 2012; Alakkas et al. 2019). The pathogenesis of NCI is incompletely understood, and host genetics is likely to play a role in individual susceptibility (Kallianpur and Levine 2014; Levine et al. 2014). Variants in iron-regulatory genes are associated with brain integrity and healthy aging (Gebril et al. 2011; Jahanshad et al. 2012). Dysregulation of iron in the brain is observed in neurodegenerative disorders, although its precise role in pathogenesis remains unclear (Hadzhieva et al. 2014). The *APOE-ε4* allele, an established risk factor for Alzheimer's disease, has been linked to the iron-transport protein ferritin within the CNS (Chang et al. 2014; Ayton et al. 2015), and recent studies support a link between *APOE-ε4* and NCI in HIV+ persons older than 60 years (Spector et al. 2010; Panos et al. 2013; Wendelken et al. 2016). Further studies of the role that genetics of host iron metabolism may play in promoting brain changes are needed in the ART era, amidst milder clinical phenotypes, and accounting for potential confounding factors. Neuroimaging endophenotypes in HIV may be more powerful outcomes for the identification of host genetic risk factors than direct measures of cognitive function, a complex phenotype which can fluctuate over short periods of time (Kallianpur and Levine 2014).

The aim of this study was to determine associations between neuroimaging measures and common variants in iron-related genes in the context of HIV infection, focusing on genes critical to iron transport and cellular and/or mitochondrial iron metabolism. The study was conducted in 243 HIV+ adults without current substance use disorder or severe (confounding) comorbid conditions, who had comprehensive neurocognitive phenotyping. Stratified analyses were also performed to detect associations specific to important HIV+ population subsets in the ART era, such as those with undetectable plasma viral load.

Methods

Study participants

Study participants included 243 HIV+ volunteers from the CNS HIV Anti-Retroviral Therapy Effects Research (CHARTER) observational study (Heaton et al. 2015), who had participated in CHARTER genetic studies and in a multicenter, prospective MRI study, as previously described (Anderson et al. 2015; Fennema-Notestine et al. 2013; Jernigan et al. 2011). Individuals with severe (confounding) comorbidities that were deemed by clinical neurologists to prevent accurate diagnosis of HIV-associated NCI were excluded, as discussed below. Recruitment and scanning of CHARTER study participants conformed to standardized protocols and took place at five U.S. sites: Johns Hopkins University (Baltimore, Maryland, $n = 37$); the Icahn School of Medicine of Mount Sinai (New York, New York, $n = 55$); the University of California at San Diego (San Diego, California, $n = 70$); the University of Texas Medical Branch (Galveston, Texas, n = 55); and the University of Washington (Seattle, Washington, $n = 26$). All procedures were approved by the Human Subjects Protection Committees of each participating institution, and written informed consent was obtained from all study participants.

Neurocognitive and psychiatric assessments

All CHARTER study participants underwent structured interviews, physical and neurological examinations, and comprehensive neurocognitive assessments, including 15 measures spanning 7 cognitive domains commonly impacted by HIV infection (Heaton et al. 2010; Heaton et al. 2011). Composite test scores (Global Deficit Score, or GDS) were derived from demographically corrected and standardized scores (T-scores) on individual test measures. NCI was defined either by a dichotomous GDS-based variable (GDS ≥ 0.5, indicating global NCI, and GDS < 0.5, considered neurocognitively unimpaired), or by well-accepted Frascati criteria for the diagnosis of HIV-associated neurocognitive disorder, which also incorporates assessment of (self)-reported functional impairment by the study participant or caregivers (Heaton et al. 2010; Heaton et al. 2011; Antinori et al. 2007). Based on a published algorithm, the presence and severity of HIV-associated neurocognitive disorder was defined by 1) the presence of impairment in at least two of seven ability domains assessed by the test battery, 2) the absence of severe (confounding) neuro-medical conditions (comorbidities), which preclude a diagnosis of NCI (e.g., ongoing substance abuse, prior stroke or cardiovascular complications without return to normal cognition after the event (Heaton et al. 2010)), and 3) assessment of functional impairment by self-report combined with performance-based criteria (Heaton et al. 2011; Antinori et al. 2007). Allowable comorbidities were chronic stable conditions deemed by experts in neurology/psychiatry to be "minimal in severity (or incidental to NCI)" or "mild-to-moderate (contributing to NCI)". We excluded individuals with "severe" (confounding) comorbid conditions that could fully explain impairment, thereby making contribution from HIV infection difficult to infer (Heaton et al. 2010); our recent work

supports worse brain integrity in this confounded category (Saloner et al. 2019).

Psychiatric diagnoses were determined using the computer-assisted Composite International Diagnostic Interview, a structured instrument widely used in psychiatric research. This tool classifies current and lifetime diagnoses of mood disorders and substance use disorders as well as other mental disorders. Current mood was also evaluated using the Beck Depression Inventory-II (Heaton et al. 2011).

Medical assessments

Medical history was gathered, structured medical and neurological examinations were performed, and blood, urine, and CSF (for those who consented to lumbar puncture) samples were collected at initial and follow-up visits. The following clinical parameters were evaluated using structured interviews and laboratory assessments, as appropriate: use of ART/history of ART use (including past exposure to older, more neurotoxic dideoxynucleoside reverse-transcriptase inhibitors, so-called "d-drugs"), detectability of HIV RNA and viral load in plasma, cluster designation (CD) 4+ T cell nadir, current CD4+ T cell count, and serologic evidence of hepatitis C virus infection, a common comorbidity that can affect the CNS (Fletcher and McKeating 2012). Plasma and CSF viral loads were quantified by reverse-transcriptase-PCR ultrasensitive assay (nominal lower quantitation limit 50 copies/mL). Nadir CD4+ T cell count was based on a combination of self-report and medical records. Current CD4+ T cell counts were measured by flow cytometry.

Neuroimaging assessments

All MRI was performed on six General Electric 1.5-Tesla scanners annually reviewed for quality at five sites; because scanner differences (e.g., hardware, software, head coil upgrades) can influence neuroimaging metrics, we included a "scanner" variable in statistical analyses to account for scanner-related effects between sites (Fennema-Notestine et al. 2007). Four series were acquired for structural morphometric analysis, including coronal two-dimensional T2- and proton-density (PD)-weighted fast spin echo sequences (section thickness = 2.0 mm), and three-dimensional sagittal T1- and PD-weighted spoiled gradient recalled acquisitions (section thickness = 1.3 mm) (Fennema-Notestine et al. 2013; Jernigan et al. 2011). Magnetic resonance spectroscopy (MRS) was performed using a standardized point-resolved spectroscopy protocol (echo time = 35 ms, repetition time = 3000 ms) (Anderson et al. 2015).

Multi-channel structural MRI As described previously (Fennema-Notestine et al. 2013; Jernigan et al. 2011), we used the multi-channel dataset in a semi-automated workflow to measure cortical, subcortical, and cerebellar gray matter; cerebellar, cerebral and abnormal (e.g., hyperintense regions on T2-weighted images) white matter; and ventricular, cerebral sulcal, and cerebellar cerebrospinal fluid, as well as supra- and infra-tentorial cranial vault volumes to account for individual differences in head size. The workflow includes image inspection for motion and other artifacts, re-slicing to a standard space, intra-subject mutual information registration, bias-correction with nonparametric non-uniformity normalization, removal of non-brain tissue, three-tissue segmentation (gray matter, white matter, and CSF), abnormal white matter designation, and anatomical labeling performed by trained anatomists. This approach includes the identification of regions of cerebral white matter with abnormal MRI signal characteristics; these regions segmented as gray matter, but are anatomically located within the white matter.

Single-voxel MRS As described previously (Anderson et al. 2015), three regional voxels were acquired: frontal gray matter (20x20x20mm and 64 acquisitions), frontal white matter (20x20x20mm and 64 acquisitions), and basal ganglia (20x20x15mm and 96 acquisitions). MRS concentrations of *N*-acetylaspartate, Choline, Myo-inositol, and Creatine were quantified using LCModel with water suppression (Provencher 2001). Water suppression allows for the examination of absolute metabolite levels, our primary measures of interest; although ratios to Creatine have been commonly reported with the aim to provide standardization across sites and studies, this approach has limitations and there is evidence that HIV infection independently affects Creatine levels directly, confounding the interpretation of ratio values and existing findings (as in Jansen et al. 2006; Anderson et al. 2015). Only metabolite estimates for appropriately placed voxels with adequate spectra (standard deviation<21) were used; therefore, sample size varied by MRS region or metabolite. Structural segmentation was used to estimate the proportion of relevant tissue volume within each MRS voxel (e.g., amount of gray matter in frontal gray matter voxel) to control for individual sampling variability.

Gene selection and genotyping

We selected 20 iron-related genes for analysis, listed in Table 1, which are known to contain common variants (i.e., minor-allele frequency ≥ 1% in a population) and are involved in one or more of the following: (a) nuclear iron storage and transport, (b) the ferroportin-hepcidin pathway, (c) mitochondrial iron transport, and/or (d) neurodegenerative phenotypes or neuronal differentiation in humans in the published literature. This gene list was not intended to be exhaustive and included only the major genes associated with iron regulation in humans, most of which have been relatively well characterized in animal or invertebrate models. We evaluated 250 single-nucleotide polymorphisms (SNPs) at these iron-

Table 1 Selected genes involved in iron metabolism, regulation, and/or transport evaluated in this study

Gene (protein)	Locus	Function and/or relevance to the CNS
HFE (hemochromatosis)	*6p21.3*	*Regulation of iron stores and hepcidin synthesis; common SNPs linked to genetic iron overload (hemochromatosis) and HIV sensory neuropathy*
HFE2 (hemojuvelin, HJV)	*1q21.1*	*Regulation of hepcidin synthesis; SNPs linked to genetic hemochromatosis*
SLC40A1 (ferroportin)	*2q32.2*	*Major regulator of macrophage iron export; immune defense*
HAMP (hepcidin)	*19q13.12*	*Master regulator of gut iron absorption and macrophage ferroportin levels (macrophage iron export)*
BMP2 (bone morphogenetic protein 2)	*20p12.3*	*Controls ferritin levels, hepcidin synthesis; neural differentiation*
BMP6 (bone morphogenetic protein 6)	*6p24–23*	*Ligand for HJV, HFE; regulates hepcidin synthesis*
TF (transferrin)	*3q22.1*	*Major cellular iron transporter in blood and brain*
TFRC (transferrin receptor 1)	*3q29*	*Receptor for transferrin, major cellular iron transport and uptake protein; hepatic iron-sensing; regulation of hepcidin and mitochondrial fusion/function*
TFR2 (transferrin receptor 2)	*7q22.1*	*Alternative transferrin receptor which mediates transferrin-bound iron uptake (and iron loading) by the liver regardless of tissue iron status; mutated in hemochromatosis type 3*
SLC11A1 (natural resistance-associated macrophage protein 1, NRAMP1)	*2q35*	*Transport of iron out of endosomes, white blood cell function*
SLC11A2 (divalent metal transporter 1)	*12q13.12*	*Encodes metal binding protein, participates in cellular iron absorption in gut; mutations result in anemia, iron overload and inflammation*
CP (ceruloplasmin)	*3q24-q25*	*Circulating plasma copper ferroxidase (Fe2 + ➔Fe3+) and iron-binding protein; homologue of hephaestin; important in glial cell iron homeostasis and neuronal survival in the CNS; mutations cause cerebellar ataxia, iron loading*
B2M (beta-2-microglobulin)	*15q21.1*	*Serum iron-binding protein and intracellular stabilizer of Hfe protein; positive acute-phase protein; involved in immune function*
ATP13A2 (ATPase iron transporter)	*1p36.13*	*Important in mitochondrial energy metabolism, resistance to toxin-induced apoptosis; mutations cause hereditary parkinsonism with dementia*
FTH1 (ferritin heavy chain)	*11q12.3*	*Ferritin subunit with ferroxidase activity, stores iron, binds Tfr1; delivers iron to oligodendrocytes*
ACO1 (cytoplasmic aconitase)	*9p21.1*	*Cytoplasmic iron-sulfur-cluster protein (iron-dependent aconitase); links cellular iron sensing to Tfr and ferritin synthesis and to the tricarboxylic acid cycle*
ACO2 (mitochondrial aconitase)	*22q13.2*	*Mitochondrial counterpart of ACO1, may be essential for mtDNA maintenance and mitochondrial iron homeostasis; interacts with FXN gene product, frataxin*
HEPH (hephaestin)	*Xq12*	*Membrane-bound ferroxidase and ceruloplasmin homologue; required for transmembrane iron transport (Fe2 + ➔Fe3+)*
FXN (frataxin)	*9q21.11*	*Mitochondrial iron transporter, delivers iron to ferrochelatase (rate-limiting step in heme synthesis)*
FTMT (mitochondrial ferritin)	*5q23.1*	*Mitochondrial iron storage molecule, regulates balance of iron between mitochondria and cytosol*

Abbreviations: Tfr, transferrin receptor (1) protein; *SNP,* single-nucleotide polymorphism; *CNS,* central nervous system; *Fe*, iron

related genetic loci of interest for which genotype data were available for CHARTER cases. Most of the SNPs evaluated in this study were very common (20–40%). Genomic DNA had previously been isolated and subjected to whole-genome genotyping using the Affymetrix™ Human SNP Array 6.0 platform, as published elsewhere (Kallianpur et al. 2014).

Quality control of genetic data Importantly, only genotypes at the selected iron-related loci, obtained from the Affymetrix array, were analyzed. However, standard quality control (QC) of genome-wide data was previously performed in all CHARTER genetics study participants and included the following steps: 1) checks for duplicates, known related individuals, and cryptic relatedness of individuals (identity-by-descent method, using a PI_HAT cut-off <0.2 to confirm non-relatedness); 2) tests of Hardy-Weinberg equilibrium (excluded SNPs had p values <1e-6); 3) checks of genetic sex; and 4) determinations of missingness (per individual and per SNP). A total of 862,089 SNPs remained following QC, including the iron-related SNPs that then were specifically selected for use in the present study. Population stratification was assessed by multidimensional scaling analysis of the N x N matrix of genome-wide, identity-by-state pairwise distances. SNPs with a minor allele frequency (MAF) <1% (11,745 SNPs) were excluded. The genotyping success rate overall was 99.7% in the cleaned (post-QC) dataset.

Statistical analyses

Since assumptions of normality for both Kolmogorov-Smirnoff and Shapiro-Wilk tests were violated for several neuroimaging variables, all measures were log-transformed prior to analyses, and the Kolmogorov-Smirnoff test was re-applied to confirm normality. The effects of numerous covariates were regressed from all neuroimaging measures to determine the need to adjust for these potentially confounding variables in multivariable regression models: covariates evaluated for inclusion were scanner, age, sex, genetic ancestry (principal components from genome-wide genetic data), education (years), Wide-Range Achievement Test score (an estimate of reading ability), nadir CD4+ T cell count, HIV RNA detectability in plasma (yes/no), ART (on vs. off), hepatitis C virus serostatus, history of d-drug use, current substance use (yes/no), estimated duration of HIV infection (months), history of diabetes mellitus (yes/no), current or lifetime history of a major depressive disorder, current or lifetime history of alcohol abuse, and comorbidity (minimal vs. mild-to-moderate and contributory to NCI). Because scanner differences (e.g., hardware, software, head coil upgrades) influence neuroimaging metrics, we included a "scanner" variable (six levels, one for each scanner at five sites, one site having two scanners) in statistical analyses to account for scanner-related differences between study sites (Fennema-Notestine et al. 2007).

A generalized linear model multivariable analysis of covariance (MANCOVA) was used to evaluate associations between continuous (log-transformed) neuroimaging measures and genotype at each locus using PLINK and unbiased, additive allelic models. Corresponding relevant neuroimaging covariates were included in all uni- and multi-variable regression models of neuroimaging outcomes: 1) for MRS, the proportion of relevant tissue volume within each voxel (e.g., amount of gray matter in frontal gray matter) to control for individual variability, thereby improving sensitivity for detection of genetic effects (Anderson et al. 2015), and 2) for structural MRI, either supra- (for cerebral measures) or infra- (for cerebellar measures) tentorial vault size to account for variation associated with individual differences in head size (Jernigan et al. 2011). Due to adjustment for cranial vault size in all models, we did not additionally adjust for sex.

All regression models were adjusted for age, nadir CD4+ T cell count, the first three ancestry principal components, scanner, and plasma HIV RNA detectability, as well as for specific covariates that were found to be significantly associated ($p < 0.05$) with individual neuroimaging measures in univariate analyses (Online Resource Tables ESM-1 and ESM-2). Analyses of frontal white matter *N*-acetylaspartate and Choline, basal ganglia *N*-acetylaspartate and Creatine, total white matter, sulcal CSF, and cerebellar white matter and gray matter included only the covariates mentioned. Since most people with HIV infection and access to ART have asymptomatic NCI or are cognitively unimpaired, and the etiology of NCI is most perplexing among relatively healthy individuals with suppressed viremia, we also tested the hypotheses that iron-related genes modulate the risk of NCI in these subsets. Analyses were therefore stratified by 1) plasma HIV RNA detectability (in which case models in the subgroup with detectable HIV RNA were adjusted for HIV RNA load), 2) presence or absence of NCI (GDS ≥ 0.5 or < 0.5, respectively), and 3) comorbidity level (absent/minimal vs. mild-to-moderate). All statistical analyses were conducted using either SAS or R software.

The linkage disequilibrium structure and number of haplotype blocks (effective independent statistical tests per genomic region) were determined using Haploview: the 250 selected SNPs fell into 37 haplotype blocks. Two levels of correction for multiple testing were therefore applied: 1) correction for the 37 haplotype blocks analyzed (significance level $p < 0.00135$), and 2) additional correction for 21 neuroimaging measures evaluated (significance level $p < 6.43\text{e-}5$). Bonferroni corrections were not deemed appropriate due to the known interdependence and coordinated regulation of many iron-related genes (Hentze et al. 2010; Kuhn 2015).

We estimated a priori that the proposed study of 250 individuals with available data would have 80% power to detect an additive genetic association model explaining 2.5% of the variance in a neuroimaging measure at an uncorrected p value <0.05 (or 3.2% of the variance at an overly conservative, Bonferroni-corrected p value <0.00014), assuming 350 SNP tests. Based on evidence from the Alzheimer's disease neuroimaging genetics literature, for disease-associated genes with small odds ratios (1.15 or less), we predicted the ability to detect effect sizes accounting for approximately 5% of the variance in a disease-related quantitative neuroimaging measure.

Results

Baseline characteristics of study participants across all neuroimaging measures, and among neurocognitively impaired and unimpaired individuals, are presented in Table 2. The mean age of the group was 44 years, and 81% were male. Self-reported race/ethnicity was 43.6% non-Hispanic white, 44.4% black, 10.3% Hispanic, and 1.6% "other". Approximately 77% of individuals were receiving ART at the time of neurocognitive assessment and neuroimaging, and 54% had a history of d-drug exposure; mean estimated duration of HIV infection was 132 months. HIV RNA was detectable in plasma in 49%. Comorbidities were deemed mild-to-moderate (and contributory to NCI) in 31%. A few individuals (3.3%) reported current substance dependency or abuse, and 53% had a lifetime history of an alcohol dependency or abuse disorder. A history of a major depressive disorder was present in 53%, and approximately 10% had a documented diagnosis of diabetes mellitus. Associations between demographic and clinical characteristics

Table 2 Demographic and HIV disease characteristics stratified by presence of neurocognitive impairment (NCI)

		GDS-Defined neurocognitive impairment	
		Not Impaired (N = 167)	*Impaired (N = 76)*
Age (years)		43.2 (8.0)	46.1 (7.1)
Education (years)		12.7 (2.3)	13.6 (2.4)
Sex (% Women)		28 (16.8%)	18 (23.7%)
Estimated Duration of HIV Infection (months)		126 (60,184)	165 (66,198)
Race/Ethnicity (Self-reported)	White	71 (43%)	35 (46%)
	Black	81 (48%)	27 (35%)
	Hispanic	13 (8%)	12 (16%)
	Other	2 (1%)	2 (3%)
Nadir CD4+ T Cell Count ($\times 10^3/mm^3$)		150 (36, 300)	135 (18, 265)
Log_{10} (HIV RNA) in Plasma (Copies/mL)		1.76 (1.70, 4.01)	1.70 (1.70, 3.44)
HIV RNA Undetectable in Plasma[a]		80 (49%)	39 (53%)
Currently on ART[b]		121 (74%)	61 (82%)
D-Drug Use	No D-drug use	75 (46%)	31 (42%)
	Past use	71 (44%)	33 (45%)
	Currently on	17 (10%)	10 (14%)
HCV Serostatus (% Positive)		45 (27%)	16 (21%)
Diabetes Dx		15 (9%)	9 (12%)
LT MDD (% Yes)		95 (57%)	35 (46%)
LT Alcohol Use Dx		96 (57%)	35 (46%)
Current Substance Use Dx		4 (2%)	4 (5%)
WRAT		98 (90, 107)	95 (82, 102)
Comorbidity	Mild-to-moderate	42 (25%)	33 (43%)
	Absent/Minimal	125 (75%)	43 (57%)

Values shown are the mean (SD), median (IQR), or count (percentage). *Abbreviations: GDS,* global deficit score; *SD,* standard deviation; *IQR,* interquartile range*; WRAT*, wide-range achievement test (measure of reading comprehension); *LLQ*, lower limit of quantitation (of assay); *HCV*, hepatitis C virus seropositivity; *ART*, antiretroviral therapy; *D-drug*, dideoxynucleoside analog drug; *LT MDD*, lifetime history of a major depressive disorder; *Dx*, diagnosis of alcohol or other substance use diagnoses encompass diagnoses of current or lifetime (mostly remote) history of abuse or dependency disorder

[a] 3 impaired and 4 unimpaired persons did not have this data available

[b] 2 impaired and 4 unimpaired persons did not have this data available

for MRS (Online Resource Table ESM-1) and structural MRI volumes (Online Resource Table ESM-2) are provided in supplemental materials.

Results of neuroimaging-genotype analyses in the entire CHARTER study population, as well as stratified analyses, are summarized in Fig. 1. Twenty-seven SNPs in 12 of the genes evaluated were significantly associated with one or more structural and/or metabolic neuroimaging measures in multivariable-adjusted analyses after applying the correction for the 37 haplotype blocks represented ($p < 0.00135$). Eight of these associations were observed in analyses that included all 243 study participants (Table 3). SNP rs7576974 (*T* allele) in the *SLC11A1* gene was associated with higher frontal gray matter *N*-acetylaspartate, and this association remained significant after applying both levels of multiple-testing correction ($p < 6.43e^{-5}$); SNP rs13358715_*T* in *FTMT* was associated with lower frontal gray matter *N*-acetylaspartate ($p = 0.0011$). Higher cortical gray matter volume was associated with *ACO1* SNP rs2026739_*G* ($p = 0.0012$) and *FXN* SNP rs11145403_*G* ($p = 8.95e^{-4}$). *BMP6* SNP rs9505293_*T* was associated with lower cerebellar gray matter volume ($p = 4.92e^{-4}$) and *FXN* SNP rs11145043_*G* with higher sulcal CSF volume ($p = 6.87e^{-4}$). Two SNPs, *BMP6* rs7454156_*G* and *ACO1* rs16918276_*T*, were associated with higher basal ganglia Creatine ($p = 7.33e^{-4}$ and $2.94e^{-4}$, respectively).

Stratified analyses in subsets of individuals based on HIV RNA detectability in plasma, presence of NCI, and severity of comorbid conditions (minimal, or incidental to NCI vs. mild/moderate, or contributing to NCI), were also performed (Fig. 1 and Table 4). Analyses stratified by plasma virus detectability yielded five SNP associations in three genes (*SLC40A1, BMP6,* and *FTMT*) among 119 individuals with undetectable virus and 3 significant SNP associations spanning three genes (*TFRC*, *BMP6*, and *FXN*) in those with detectable viremia ($n = 117$). Among individuals with NCI ($n = 76$), six SNPs in four genes (*ACO1*, *BMP6*, *FXN*, and *TF*)

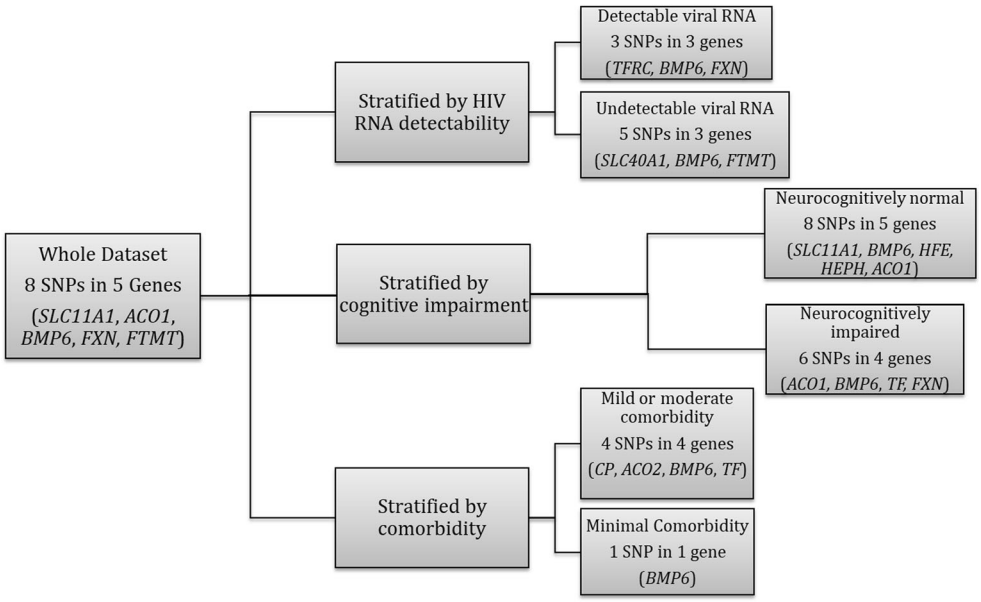

Fig. 1 Summary of Iron-related genes in which SNPs were significantly associated with neuroimaging measures after corrections for multiple statistical tests. *Abbreviations: SNPs*, single-nucleotide polymorphisms; *FXN*, frataxin; *TFRC*, transferrin receptor 1; *TF,* transferrin; *SLC11A1,* natural resistance-associated macrophage protein 1; *BMP6*, bone morphogenetic protein 6; *FTMT*, mitochondrial ferritin; *SLC40A1*, ferroportin; *HEPH*, hephaestin; *HFE*, hemochromatosis (1) gene; *CP,* ceruloplasmin; *ACO1*, cytoplasmic aconitase; *ACO2*, mitochondrial aconitase; *CP*, ceruloplasmin; *TF*, transferrin

were statistically significant; among 167 neurocognitively normal individuals, eight SNP associations in five genes (*ACO1*, *BMP6*, *HEPH*, *HFE*, and *SLC11A1*) were detected. Stratification by comorbidity level (absent/minimal vs. mild-to-moderate) yielded four significant SNPs in four genes (*ACO2*, *BMP6*, *CP*, and *TF*) in individuals with mild-to-moderate comorbidities and a single SNP in *BMP6* in the subgroup with absent/minimal comorbid conditions. Minor allele frequencies of significantly associated variants ranged from 0.014 to 0.461. Adjusted *beta* coefficients from multivariable regression models and odds ratios for the coded alleles using a dominant genetic model are presented in Online Resource Table ESM-3 for statistically significant SNPs that survived both levels of correction. Of note, alleles rs13404407_*C* in *SLC40A1* (ferroportin) and rs9611598_*A* in *ACO2* (mitochondrial aconitase) were present at less than 5% frequency in the study sample.

Discussion

To our knowledge, this study represents the first to associate genes involved in iron metabolism, transport and/or regulation with neuroimaging measures in the context of HIV infection, and one of very few studies examining these associations in

Table 3 Multivariable-adjusted SNP associations with neuroimaging measures in all 243 HIV+ study participants

Gene	SNP (coded allele)	Type of variant	# Neuroimaging measures nominally associated ($p < 0.05$)	Neuroimaging measure(s)	Direction of effect	*p* value	MAF
SLC11A1	*rs7576974 (T)*	*Intronic/5'UTR*	*8*	*Frontal GM - NAA*	*Higher*	***3.62e-5***	*0.066*
BMP6	*rs9505293 (T)*	*Intronic*	*23*	*Cerebellar GM*	*Lower*	*4.92e-4*	*0.138*
	rs7454156 (G)	*Intronic*	*15*	*BG - Cr*	*Higher*	*7.33e-4*	*0.175*
ACO1	*rs2026739 (G)*	*Intronic*	*13*	*Cortical GM*	*Higher*	*1.16e-3*	*0.339*
	rs16918276 (T)	*Intronic*	*20*	*BG - Cr*	*Higher*	*2.94e-4*	*0.109*
FXN	*rs2498434 (G)*	*Intronic*	*16*	*Sulcal CSF*	*Higher*	*6.87e-4*	*0.495*
	rs11145043 (G)	*Intronic/3'UTR*	*9*	*Cortical GM*	*Higher*	*8.95e-4*	*0.366*
FTMT	*rs13358715 (T)*	*Intronic*	*10*	*Frontal GM - NAA*	*Lower*	*1.07e-3*	*0.054*

All associations that survived the first level of multiple-testing correction for number of haplotype blocks evaluated ($p < 0.00135$) are shown; the single SNP that survived both levels of correction (for 37 haplotype blocks and 21 neuroimaging measures, $p < 6.43e\text{-}5$) is shown in **bold**

Abbreviations: GM, gray matter; *WM*, white matter; *BG*, basal ganglia; *Cr*, creatine; *CSF*, cerebrospinal fluid; *NAA*, *N*-acetylaspartate; *SLC11A1*, natural resistance-associated macrophage protein 1; *BMP6*, bone-morphogenetic protein 6, *ACO1*, cytoplasmic aconitase; *FXN*, frataxin; *FTMT*, mitochondrial ferritin; *OR*, odds ratio; *MAF*, minor allele frequency

Table 4 Summary of multivariable-adjusted SNP associations with neuroimaging measures in analyses stratified by plasma HIV RNA detectability, comorbidity (mild-to-moderate vs. absent/minimal), and presence of GDS-defined neurocognitive impairment

Study stratum	Gene	SNP (coded allele)	Type of variant	Neuroimaging measure(s)	*p*-value	MAF
Undetectable Plasma HIV RNA (*n* = 119)	*SLC40A1*	rs13404407 (C)	Intronic	Abnormal WM	**2.23e-6**	0.029
	BMP6	rs11243204 (G)	Intronic	Sulcal CSF	8.81e-5	0.158
	BMP6	rs11760020 (T)	Intronic	Sulcal CSF	4.37e-4	0.249
	BMP6	rs267807 (A)	Intronic	Subcortical GM	1.11e-3	0.395
	FTMT	rs13358715 (T)	Intronic	Frontal WM - NAA	1.24e-3	0.054
Detectable Plasma HIV RNA (n=117[a])	*TFRC*	rs17091382 (A)	Intronic	Subcortical GM	**3.23e-5**	0.060
	BMP6	rs7454156 (G)	Intronic	BG - Cr	7.65e-4	0.175
	FXN	rs2498434 (G)	Intronic	Sulcal CSF	5.13e-4	0.495
Minimal Comorbidity (*n* = 168)	*BMP6*	rs752751 (T)	Intronic	Frontal GM - Cr	8.99e-4	0.477
Mild or Moderate Comorbidity (*n* = 75)	*CP*	rs4974389 (A)	Intronic	BG - Cho	**3.52e-5**	0.382
	ACO2	rs9611598 (A)	Intronic	Subcortical GM	**5.94e-5**	0.023
				Cerebellar GM	6.84e-4	
	BMP6	rs1358893 (T)	Intronic	Abnormal WM	7.02e-4	0.356
	TF	rs7633232 (C)	Intronic	Frontal GM - Cho	2.52e-4	0.014
				Frontal GM - Cr	6.33e-4	
Neurocognitively Normal (n = 167)	*SLC11A1*	rs7576974 (T)	Intronic/5'UTR	Frontal GM - NAA	**3.62e-5**	0.066
	BMP6	rs1107495 (G)	Upstream 2 KB	Frontal WM - Cr	2.19e-4	0.191
	BMP6	rs9505293 (T)	Intronic	Cerebellar GM	9.10e-4	0.138
	BMP6	rs7454156 (G)	Intronic	BG - MI	5.68e-4	0.175
				BG - Cr	1.13e-3	
	BMP6	rs11960697 (A)	Intronic	Abnormal WM	7.46e-4	0.019
	HFE	rs1800562 (A)	Missense	Cerebellar GM	3.98e-4	0.033
	HEPH	rs7059116 (A)	Intronic	Frontal WM - MI	1.40e-4	0.111
	ACO1	rs2026739 (G)	Intronic	Frontal WM - NAA	1.70e-4	0.339
Neurocognitively impaired (n = 76)	*ACO1*	rs3780474 (G)	Intronic	Subcortical GM	2.81e-4	0.418
	BMP6	rs9505293 (T)	Intronic	Cerebellar GM	4.92e-4	0.138
	TF	rs2718796 (G)	Intronic	Abnormal WM	1.03e-3	0.023
	TF	rs8177238 (G)	Missense	Frontal WM Cho	1.11e-3	0.023
	TF	rs8177241 (T)	Intronic	Frontal WM Cho	1.11e-3	0.027
	FXN	rs10126006 (A)	Intronic	Cortical GM	5.11e-4	0.346

Only *p* values for SNP associations that survived at least one level of multiple-testing correction ($p < 0.00135$ and $p < 0.00006435$) are shown, and those SNPs meeting two levels of correction are **bolded**

Abbreviations: WM, white matter; *GM*, gray matter; *NAA*, *N*-acetylaspartate; *Cr*, Creatine; *Cho*, Choline; *CSF*, cerebrospinal fluid; *GDS*, Global Deficit Score; *MAF*, minor allele frequency

[a] Viral load measurements were not available for all participants

humans more broadly. Although iron dysregulation has been consistently linked to neurodegenerative disorders, few studies have investigated the contribution of variation in iron-related genes to metabolic or structural brain characteristics (Gebril et al. 2011; Jahanshad et al. 2012; Gazzina et al. 2016). Furthermore, five SNP associations that we observed in this diverse population of HIV+ individuals remained significant following *p* value adjustment for multiple statistical tests, including adjustment for the number of distinct haplotypes and neuroimaging measures that were evaluated.

One of these SNPs, rs7576974_*T*, is located in *SLC11A1*, a gene which is responsible for macrophage-monocyte iron recycling and encodes a key macrophage antimicrobial resistance protein, also known as Nramp1. This SNP was associated with higher frontal gray matter *N*-acetylaspartate among all study participants, as well as within the unimpaired subset. Other SNPs in this gene are known to be associated with either increased or decreased risk of autoimmune and infectious disorders, and a nearby SNP in *SLC11A1* was linked to reduced autoimmune inflammation (Archer et al. 2015). Given that *N*-acetylaspartate is a marker of neuronal integrity and is lower in the setting of HIV infection (Harezlak et al. 2011; Cysique et al. 2018), we postulate that this SNP is neuroprotective in HIV+ persons. *SLC11A1* genotypes have been linked to mortality in

HIV infection (McDermid et al. 2009). While stratified analyses are not generally held to the same standard of multiple-testing correction, this SNP in *SLC11A1* also met a third level of correction for the three hypotheses tests involved in stratified analyses (significant *p* value threshold <2.14e-5). The Slc11A1 protein, along with ferroportin and the transferrin receptor (encoded by *SLC40A1* and *TFRC*, respectively), constitute major proteins of the innate immune response (Johnson and Wessling-Resnick 2012; Archer et al. 2015). *SLC11A1* regulates macrophage activation and has been associated with incident mycobacterial infection; this gene may also modulate neuroinflammation in HIV clade B infection and was linked to HIV-related mortality among untreated persons living with HIV in West Africa (Li et al. 2011; Yndart et al. 2015; McDermid et al. 2009).

Additional analyses also revealed other statistically significant SNPs that survived multiple-testing correction, in genes with important roles in iron regulation and transport. SNP rs13404407_*C* in ferroportin (*SLC40A1* gene), despite being present at low frequency (3%) in our study population, was associated with a 2.5-fold higher volume of abnormal white matter in aviremic individuals. Other SNPs, including rs17091382_*A* in the transferrin receptor gene (*TFRC*) and rs9611598_*A* in mitochondrial aconitase (*ACO2* gene), showed suggestive associations with less subcortical gray matter (adjusted odds ratio 0.90 in individuals with detectable plasma virus, and odds ratio 0.73 among those with significant comorbidity, respectively). Finally, SNP rs4974389_*A* in *CP* was associated with increased basal ganglia Choline, a marker of inflammation and increased membrane turnover (Young et al. 2014). Importantly, like the SNP rs7576974_*T* in *SLC11A1*, we note that the SNP in *SLC40A1* (ferroportin), would also meet a more stringent *p* value threshold that accounts for the 3 strata analyzed ($p < 2.14e\text{-}5$). Nevertheless, results for this SNP must be interpreted with caution, as only 3 individuals had variant alleles at this locus in the aviremic subset. The magnitude of individual SNP effects, beyond those of ferroportin and *ACO2* genetic variants, was observed to be small.

Ferroportin is an extremely important molecule in iron metabolism and innate immunity, serving as the portal for iron entry from the gut into the bloodstream and for iron export from macrophage-monocytes to metabolically active cells in the brain, bone marrow and other tissues (Coffey and Ganz 2017). Like ferroportin, transferrin receptor 1, encoded by the *TFRC* gene, is also widely expressed on most cells within the CNS; transferrin receptor expression is essential to brain iron uptake (Gebril et al. 2011). SNPs in these genes may therefore disrupt the delicate balance between transferrin-mediated iron uptake and ferroportin-related iron export, leading to mitochondrial dysfunction and cellular oxidative stress affecting the white matter in particular. Aconitase is an iron-sulfur-cluster-containing enzyme important for its participation in the tricarboxylic acid cycle, where it catalyzes the isomerization of citrate; it is present in two forms, one localized to the cytoplasm (cytoplasmic (c)-aconitase, encoded by *ACO1*) and one to localized to the mitochondrial matrix (mitochondrial (m)-aconitase, encoded by *ACO2*) (Lushchak et al. 2014). Both isoforms also function as biosensors of reactive oxygen species and iron levels, with c-aconitase serving dual roles as an iron-regulatory protein (IRP-1) that post-transcriptionally regulates the synthesis of transferrin receptor and ferritin, depending on ambient iron levels. Iron levels also appear to regulate the expression of aconitases; hence, these proteins serve to intimately link iron metabolism to cellular energy requirements. Iron metabolism is altered by HIV infection, and decreased serum citrate levels, possibly reflecting altered aconitase activity, have been documented in HIV+ persons compared to seronegative controls (Pugliese et al. 2002). Furthermore, CSF metabolomics studies have documented an association between worsening neurocognitive function in HIV infection and a shift to aerobic glycolysis, accompanied by elevated CSF citrate and acetate levels, in the absence of changes in plasma viral load (Dickens et al. 2015). Decreases in the expression of c-aconitase, ceruloplasmin, and possibly, ferroportin, have also been suggested to lead to impairment of cellular iron export and oxidative stress in Alzheimer's disease (Guerreiro et al. 2015). M-aconitase activity in peripheral blood lymphocytes is significantly reduced in patients with Alzheimer's disease and mild cognitive impairment (Mangialasche et al. 2015). We previously identified effects of *ACO1* SNP rs2026739 on neuropathic pain severity in HIV+ CHARTER study participants (Kallianpur et al. 2014). This c-aconitase SNP and two other mitochondrial iron transporters, frataxin and mitochondrial ferritin (encoded by *FXN* and *FTMT*, respectively) were also associated with neuroimaging measures after the first level of multiple-testing correction. Interestingly, frataxin is believed to be important in shuttling iron between c-aconitase and IRP-1 (Lushchak et al. 2014).

Given that both HIV-associated neurocognitive disorder and neuroimaging abnormalities develop and/or progress in only a subset of HIV+ individuals (Harezlak et al. 2011; Cysique et al. 2018; Heaton et al. 2010), there has been longstanding debate as to the contribution of host genetic differences. In this study of chronically HIV+ adults, we identified a total of 27 iron-regulatory genes harboring SNPs that were significantly associated with neuroimaging measures in multivariable models, either in the entire sample, or in a subset. We found that SNP rs9611598_*A* in *ACO2* was associated with higher basal ganglia Choline. The association of this SNP in a gene involved in mitochondrial iron regulation and glycolytic metabolism with Choline, a marker that is elevated in the brain during HIV infection (Harezlak et al. 2011), may indicate pro-inflammatory cellular effects. Lastly, SNPs in at least three genes were associated with changes in regional brain volumes. Iron excess has been associated with brain atrophy in other neurological and systemic disorders

(Gazzina et al. 2016; Chai et al. 2015). Therefore, these SNPs may modulate the risk of regional (e.g., subcortical) brain atrophy, which is commonly observed in HIV+ individuals and associated with NCI (Nir et al. 2014).

Iron homeostasis is essential for maintenance of mitochondrial function and energy production in the brain, as neural tissues have extremely high metabolic demand, and iron is a key component of the molecular complexes that constitute the electron transport chain. Furthermore, by virtue of its ability to readily accept and donate electrons, iron is a required cofactor for a very large number of fundamental metabolic processes, including synthesis of DNA, heme, monoamine neurotransmitters, and myelin (Kallianpur et al. 2014; Patton et al. 2017; Puig et al. 2017). However, iron that is not tightly protein-bound is highly reactive and generates oxidative stress by catalyzing free radical reactions. While studies in neonates and adolescents have demonstrated lasting and often irreversible alterations of brain structure and cognitive ability following iron deficiency early in life, the impact of both iron deficiency and iron excess on brain integrity and function in adults is considerably less well understood (Georgieff 2011; Belaidi and Bush 2016). Iron present in excess or reactive forms is also directly injurious, leading to neuronal death (Belaidi and Bush 2016). Brain iron regulation is altered in several common neurodegenerative disorders, including Alzheimer's disease, Parkinson's disease, which involve abnormal concentrations of iron in specific brain regions on neuroimaging studies (Georgieff 2011; Pichler et al. 2013; Crespo et al. 2014). Brain iron content has been associated with specific brain structures on MRI in healthy and aging individuals, including the basal ganglia and thalamus, and serum iron is associated with neuroimaging characteristics of these brain regions, as well as the hippocampus (Jahanshad et al. 2012). Jahanshad et al. (Jahanshad et al. 2012) found that in healthy young adults, fractional anisotropy, a measure of brain white matter integrity estimated from diffusion tensor imaging scans of the brain, was associated with serum levels of the major iron transport protein transferrin, measured years earlier during adolescence.

Lower transferrin levels were associated with higher fractional anisotropy, suggesting greater brain integrity. Brain iron normally increases with age, and both common and rare genetic variants that affect iron transport are associated with brain iron accumulation (Bettencourt et al. 2016). Age-related white matter lesions in HIV-seronegative persons have also been associated with increased ferric iron staining and a pattern of decreased cellular iron influx, and increased export of iron from cells was noted in messenger RNA expression studies using quantitative PCR (Gebril et al. 2011). White matter lesions, or abnormal white matter, are common among HIV+ individuals and have been inconsistently associated with neurocognitive deficits, even in aviremic persons (Gongvatana et al. 2009; Alakkas et al. 2019). Abnormal white matter increases with age and is more likely to be associated with a history of severe immunosuppression, as indicated by the CD4+ T cell count (Fennema-Notestine et al. 2013). Synaptodendritic loss and microstructural damage to white matter are also characteristic of HIV infection in the current ART era (Kallianpur and Levine 2014).

Neuroimaging abnormalities may occur early in HIV infection, regardless of NCI, but few studies have documented changes in brain iron distribution (Granziera et al. 2013). The putamen may be more susceptible to these early HIV-mediated changes (Wright et al. 2016). Granziera et al. (Granziera et al. 2013) used more iron-sensitive imaging techniques to show that loss of structural integrity could be demonstrated in global white matter, cortical gray matter, thalamus, and basal ganglia in HIV+ persons with mild neurocognitive disorders and undetectable HIV RNA in plasma relative to healthy controls, and most of these alterations were more pronounced than in unimpaired HIV+ persons. In all HIV+ persons, T1 relaxation times were generally shorter (and T2* longer) than in healthy controls, likely reflecting *lower* iron content. The imaging measures used, however, were not specific for iron. Older studies have suggested increased brain iron deposition in the basal ganglia of HIV+ persons, as in older HIV-seronegative persons, particularly in the globus pallidus and putamen (Miszkiel et al. 1997; Wright et al. 2016). Soon after seroconversion, MRS metabolites also are affected with changes that correlate with inflammation and neuronal injury. HIV-related effects are generally observed in subcortical (basal ganglia) and cortical (frontal and parietal) gray matter as well as within the white matter, compared to HIV-seronegative individuals. Furthermore, HIV+ persons tend to have lower *N*-acetylaspartate and higher Choline and Myo-inositol levels, with more severe effects reported in cognitively impaired individuals. While ART ameliorates these changes and can improve neurocognitive function, MRS metabolite levels generally do not normalize.

We acknowledge the limitations of this study, despite several strengths. Neuroimaging methods sensitive to iron status were not performed: studies incorporating T2*, susceptibility-weighted imaging, and other methods of iron-sensitive neuroimaging are underway. R2* relaxometry has been validated as a means to quantify brain iron and should therefore also receive consideration in future studies. The list of genes involved in iron homeostasis is extremely large, and the 20 genes studied here represent only a small fraction of polymorphic genes that may be important in brain structure and metabolism. Genes such as *ACO1, SLC40A1,* and *HFE* have previously been associated with neurocognitive disorders and/or neurodegeneration (Crespo et al. 2014; Jahanshad et al. 2012). *HFE* C187G genotypes, which have been previously linked to other neurocognitive disorders, were not available for these analyses. Associations involving SNPs in *TFRC*, *CP*, and *SLC11A1* were statistically robust, but due to very small numbers of variant alleles, findings for SNPs in *SLC40A1* and *ACO2* must be

considered exploratory, requiring further study to determine if the observed associations persist in other HIV+ and HIV seronegative populations. Due to the presence of 2 minor alleles in only one individual at the *SLC11A1* SNP locus, the impact of allele dosage could not be assessed. Replication of our findings in larger numbers of individuals with and without HIV, and exploration of iron-related mechanisms of NCI, are therefore needed. Furthermore, although we excluded severely confounded cases and adjusted our analyses for a number of potentially confounding variables, we cannot eliminate the possibility of residual confounding; factors such as neuropsychiatric or substance abuse variables might also be associated with iron metabolism. Although the vast majority of substance use variables in this cohort were previously shown to be unrelated to cognitive function (Byrd et al. 2011), our findings may not generalize to people with HIV infection who also have heavy or longstanding substance use. Finally, the generalizability of these neuroimaging-genetic findings to other HIV-seropositive cohorts, and their link to HIV neuropathogenesis specifically, as well as exploration of similar associations in HIV-seronegative populations, remains to be determined in future studies. Therefore, these results should be interpreted within the context of HIV and may or may not be due to HIV infection. Nevertheless, the multi-center design of this study, the diversity of the study population, and the persistence of significant associations after correcting for the number of evaluated genetic haplotypes and neuroimaging measures, support the validity of these findings and their generalizability to many people with HIV.

Acknowledgements This work was supported in part by awards from National Institutes of Health (R01 MH095621, T. Hulgan and A. Kallianpur; K24 MH097673, S.L. Letendre; the CNS HIV Anti-Retroviral Therapy Effects Research (CHARTER) N01 MH22005 and HHSN271201000036C, to I. Grant; R01 MH107345, R.K. Heaton and S.L. Letendre; and P30 MH062512, R. Heaton). The views expressed in this article are those of the authors and do not reflect the official policy or position of the United States Government. We gratefully acknowledge all individuals who participated in CHARTER studies, as well as all CHARTER study investigators*.

**The CNS HIV Anti-Retroviral Therapy Effects Research was supported by awards N01 MH22005, HHSN271201000036C and HHSN271201000030C from the National Institutes of Health.* The CNS HIV Anti-Retroviral Therapy Effects Research (CHARTER) group is affiliated with Johns Hopkins University; the Icahn School of Medicine at Mount Sinai; University of California, San Diego; University of Texas, Galveston; University of Washington, Seattle; Washington University, St. Louis; and is headquartered at the University of California, San Diego and includes: Director: Igor Grant, M.D.; Co-Directors: Scott L. Letendre, M.D., Ronald J. Ellis, M.D., Ph.D., Thomas D. Marcotte, Ph.D.; Center Manager: Donald Franklin, Jr.; Neuromedical Component: Ronald J. Ellis, M.D., Ph.D. (P.I.), J. Allen McCutchan, M.D.; Laboratory and Virology Component: Scott Letendre, M.D. (Co-P.I.), Davey M. Smith, M.D. (Co-P.I.).; Neurobehavioral Component: Robert K. Heaton, Ph.D. (P.I.), J. Hampton Atkinson, M.D., Matthew Dawson; Imaging Component: Christine Fennema-Notestine, Ph.D. (P.I.), Michael J Taylor, Ph.D., Rebecca Theilmann, Ph.D.; Data Management Component: Anthony C. Gamst, Ph.D. (P.I.), Clint Cushman; Statistics Component: Ian Abramson, Ph.D. (P.I.), Florin Vaida, Ph.D.; Johns Hopkins University Site: Ned Sacktor (P.I.), Vincent Rogalski; Icahn School of Medicine at Mount Sinai Site: Susan Morgello, M.D. (Co-P.I.) and David Simpson, M.D. (Co-P.I.), Letty Mintz, N.P.; University of California, San Diego Site: J. Allen McCutchan, M.D. (P.I.); University of Washington, Seattle Site: Ann Collier, M.D. (Co-P.I.) and Christina Marra, M.D. (Co-P.I.), Sher Storey, PA-C.; University of Texas, Galveston Site: Benjamin Gelman, M.D., Ph.D. (P.I.), Eleanor Head, R.N., B.S.N.; and Washington University, St. Louis Site: David Clifford, M.D. (P.I.), Muhammad Al-Lozi, M.D., Mengesha Teshome, M.D.

Data availability statement These anonymized, de-identified derived datasets generated during and/or analyzed during the current study are available from the corresponding author on reasonable request.

Funding This study was supported in part by awards from National Institutes of Health (R01 MH095621, T. Hulgan and A. Kallianpur; K24 MH097673, S.L. Letendre; the CNS HIV Anti-Retroviral Therapy Effects Research (CHARTER) N01 MH22005 and HHSN271201000036C, to I. Grant; R01 MH107345, R.K. Heaton and S.L. Letendre; and P30 MH062512, R. Heaton). The views expressed in this article are those of the authors and do not reflect the official policy or position of the United States Government.

Compliance with ethical standards

All procedures performed in studies involving human participants were in accordance with the ethical standards of the institutional and/or national research committee and with the 1964 Helsinki declaration and its later amendments or comparable ethical standards.

Conflict of interest The authors report no biomedical financial interests or potential conflicts of interest relevant to this manuscript beyond those participating through the NIH funding stated above.

Christine Fennema-Notestine, PhD[1,2] has no disclosures to report, other than participating through NIH funding stated above.

Tricia A. Thornton-Wells, PhD[3] has no disclosures to report, other than participating through NIH funding stated above.

Todd Hulgan, PhD[4] has no disclosures to report, other than the NIH funding stated above.

Scott Letendre, MD[5] has no disclosures to report, other than the NIH funding stated above.

Ronald J. Ellis, MD, PhD[6] has no disclosures to report, other than participating through NIH funding stated above.

Donald R. Franklin, Jr., BS[1] has no disclosures to report, other than participating through NIH funding stated above.

Albert M. Anderson, MD[7] has no disclosures to report.

Robert K. Heaton, PhD[1] has no disclosures to report, other than the NIH funding stated above.

Cinnamon S. Bloss, PhD[1,8] has no disclosures to report.

I. Grant, MD[1] has no disclosures to report, other than the NIH funding stated above.

Asha R. Kallianpur, MD, MPH[9,10] has no disclosures to report, other than the NIH funding stated above.

Informed consent Informed consent was obtained from all individual participants included in the study.

References

Alakkas, A., Ellis, R. J., Watson, C. W., Umlauf, A., Heaton, R. K., Letendre, S., et al. (2019). White matter damage, neuroinflammation, and neuronal integrity in HAND. *Journal of Neurovirology, 25*(1), 32–41. https://doi.org/10.1007/s13365-018-0682-9.

Anderson, A. M., Fennema-Notestine, C., Umlauf, A., Taylor, M. J., Clifford, D. B., Marra, C. M., et al. (2015). CSF biomarkers of monocyte activation and chemotaxis correlate with magnetic resonance spectroscopy metabolites during chronic HIV disease. *Journal of Neurovirology, 21*(5), 559–567. https://doi.org/10.1007/s13365-015-0359-6.

Antinori, A., Arendt, G., Becker, J. T., Brew, B. J., Byrd, D. A., Cherner, M., et al. (2007). Updated research nosology for HIV-associated neurocognitive disorders. *Neurology, 69*(18), 1789–1799.

Archer, N. S., Nassif, N. T., & O'Brien, B. A. (2015). Genetic variants of SLC11A1 are associated with both autoimmune and infectious diseases: Systematic review and meta-analysis. *Genes and Immunity, 16*(4), 275–283. https://doi.org/10.1038/gene.2015.8.

Ayton, S., Faux, N. G., Bush, A. I., & Alzheimer's Disease Neuroimaging, I. (2015). Ferritin levels in the cerebrospinal fluid predict Alzheimer's disease outcomes and are regulated by APOE. *Nature Communications, 6*, 6760. https://doi.org/10.1038/ncomms7760.

Belaidi, A. A., & Bush, A. I. (2016). Iron neurochemistry in Alzheimer's disease and Parkinson's disease: Targets for therapeutics. *Journal of Neurochemistry, 139*(Suppl 1), 179–197. https://doi.org/10.1111/jnc.13425.

Bettencourt, C., Forabosco, P., Wiethoff, S., Heidari, M., Johnstone, D. M., Botia, J. A., et al. (2016). Gene co-expression networks shed light into diseases of brain iron accumulation. *Neurobiology of Disease, 87*, 59–68. https://doi.org/10.1016/j.nbd.2015.12.004.

Byrd, D. A., Fellows, R. P., Morgello, S., Franklin, D., Heaton, R. K., Deutsch, R., et al. (2011). Neurocognitive impact of substance use in HIV infection. *Journal of Acquired Immune Deficiency Syndromes, 58*(2), 154–162. https://doi.org/10.1097/QAI.0b013e318229ba41.

Chai, C., Zhang, M., Long, M., Chu, Z., Wang, T., Wang, L., et al. (2015). Increased brain iron deposition is a risk factor for brain atrophy in patients with haemodialysis: A combined study of quantitative susceptibility mapping and whole brain volume analysis. *Metabolic Brain Disease, 30*(4), 1009–1016. https://doi.org/10.1007/s11011-015-9664-2.

Chang, Y. L., Fennema-Notestine, C., Holland, D., McEvoy, L. K., Stricker, N. H., Salmon, D. P., et al. (2014). APOE interacts with age to modify rate of decline in cognitive and brain changes in Alzheimer's disease. *Alzheimers & Dementia, 10*(3), 336–348. https://doi.org/10.1016/j.jalz.2013.05.1763.

Coffey, R., & Ganz, T. (2017). Iron homeostasis: An anthropocentric perspective. *The Journal of Biological Chemistry, 292*(31), 12727–12734. https://doi.org/10.1074/jbc.R117.781823.

Crespo, A. C., Silva, B., Marques, L., Marcelino, E., Maruta, C., Costa, S., et al. (2014). Genetic and biochemical markers in patients with Alzheimer's disease support a concerted systemic iron homeostasis dysregulation. *Neurobiology of Aging, 35*(4), 777–785. https://doi.org/10.1016/j.neurobiolaging.2013.10.078.

Cysique, L. A., Juge, L., Gates, T., Tobia, M., Moffat, K., Brew, B. J., et al. (2018). Covertly active and progressing neurochemical abnormalities in suppressed HIV infection. *Neurol Neuroimmunol Neuroinflamm, 5*(1), e430. https://doi.org/10.1212/NXI.0000000000000430.

Dickens, A. M., Anthony, D. C., Deutsch, R., Mielke, M. M., Claridge, T. D., Grant, I., et al. (2015). Cerebrospinal fluid metabolomics implicate bioenergetic adaptation as a neural mechanism regulating shifts in cognitive states of HIV-infected patients. *AIDS, 29*(5), 559–569. https://doi.org/10.1097/QAD.0000000000000580.

Fennema-Notestine, C., Gamst, A. C., Quinn, B. T., Pacheco, J., Jernigan, T. L., Thal, L., et al. (2007). Feasibility of multi-site clinical structural neuroimaging studies of aging using legacy data. *Neuroinformatics, 5*(4), 235–245. https://doi.org/10.1007/s12021-007-9003-9.

Fennema-Notestine, C., Ellis, R. J., Archibald, S. L., Jernigan, T. L., Letendre, S. L., Notestine, R. J., et al. (2013). Increases in brain white matter abnormalities and subcortical gray matter are linked to CD4 recovery in HIV infection. *Journal of Neurovirology, 19*(4), 393–401. https://doi.org/10.1007/s13365-013-0185-7.

Fletcher, N. F., & McKeating, J. A. (2012). Hepatitis C virus and the brain. [research support, non-U.S. Gov't]. *Journal of Viral Hepatitis, 19*(5), 301–306. https://doi.org/10.1111/j.1365-2893.2012.01591.x.

Gazzina, S., Premi, E., Zanella, I., Biasiotto, G., Archetti, S., Cosseddu, M., et al. (2016). Iron in frontotemporal lobar degeneration: A new subcortical pathological pathway? *Neurodegenerative Diseases, 16*(3–4), 172–178. https://doi.org/10.1159/000440843.

Gebril, O. H., Simpson, J. E., Kirby, J., Brayne, C., & Ince, P. G. (2011). Brain iron dysregulation and the risk of ageing white matter lesions. *Neuromolecular Medicine, 13*(4), 289–299. https://doi.org/10.1007/s12017-011-8161-y.

Georgieff, M. K. (2011). Long-term brain and behavioral consequences of early iron deficiency. *Nutrition Reviews, 69*(Suppl 1), S43–S48. https://doi.org/10.1111/j.1753-4887.2011.00432.x.

Gongvatana, A., Schweinsburg, B. C., Taylor, M. J., Theilmann, R. J., Letendre, S. L., Alhassoon, O. M., et al. (2009). White matter tract injury and cognitive impairment in human immunodeficiency virus-infected individuals. *Journal of Neurovirology, 15*(2), 187–195. https://doi.org/10.1080/13550280902769756.

Granziera, C., Daducci, A., Simioni, S., Cavassini, M., Roche, A., Meskaldji, D., et al. (2013). Micro-structural brain alterations in aviremic HIV+ patients with minor neurocognitive disorders: A multi-contrast study at high field. [Research Support, Non-U.S. Gov't]. *PLoS ONE, 8*(9), e72547. https://doi.org/10.1371/journal.pone.0072547.

Guerreiro, C., Silva, B., Crespo, A. C., Marques, L., Costa, S., Timoteo, A., et al. (2015). Decrease in APP and CP mRNA expression supports impairment of iron export in Alzheimer's disease patients. *Biochim Biophys Acta, 1852*(10 Pt A), 2116–2122. https://doi.org/10.1016/j.bbadis.2015.07.017.

Hadzhieva, M., Kirches, E., & Mawrin, C. (2014). Review: Iron metabolism and the role of iron in neurodegenerative disorders. *Neuropathology and Applied Neurobiology, 40*(3), 240–257. https://doi.org/10.1111/nan.12096.

Harezlak, J., Buchthal, S., Taylor, M., Schifitto, G., Zhong, J., Daar, E., et al. (2011). Persistence of HIV-associated cognitive impairment, inflammation, and neuronal injury in era of highly active antiretroviral treatment. *AIDS, 25*(5), 625–633. https://doi.org/10.1097/QAD.0b013e3283427da7.

Heaton, R. K., Clifford, D. B., Franklin, D. R., Jr., Woods, S. P., Ake, C., Vaida, F., et al. (2010). HIV-associated neurocognitive disorders persist in the era of potent antiretroviral therapy: CHARTER study. *Neurology, 75*(23), 2087–2096. https://doi.org/10.1212/WNL.0b013e318200d727.

Heaton, R. K., Franklin, D. R., Ellis, R. J., McCutchan, J. A., Letendre, S. L., Leblanc, S., et al. (2011). HIV-associated neurocognitive disorders before and during the era of combination antiretroviral therapy: Differences in rates, nature, and predictors. *Journal of Neurovirology, 17*(1), 3–16. https://doi.org/10.1007/s13365-010-0006-1.

Heaton, R. K., Franklin, D. R., Jr., Deutsch, R., Letendre, S., Ellis, R. J., Casaletto, K., et al. (2015). Neurocognitive change in the era of HIV combination antiretroviral therapy: The longitudinal CHARTER study. *Clinical Infectious Diseases, 60*(3), 473–480. https://doi.org/10.1093/cid/ciu862.

Hentze, M. W., Muckenthaler, M. U., Galy, B., & Camaschella, C. (2010). Two to tango: Regulation of mammalian iron metabolism. *Cell, 142*(1), 24–38. https://doi.org/10.1016/j.cell.2010.06.028.

Jahanshad, N., Kohannim, O., Hibar, D. P., Stein, J. L., McMahon, K. L., de Zubicaray, G. I., et al. (2012). Brain structure in healthy adults is related to serum transferrin and the H63D polymorphism in the HFE gene. *Proceedings of the National Academy of Sciences of the*

United States of America, 109(14), E851–E859. https://doi.org/10.1073/pnas.1105543109.

Jansen, J. F., Backes, W. H., Nicolay, K., & Kooi, M. E. (2006). 1H MR spectroscopy of the brain: Absolute quantification of metabolites. [review]. *Radiology, 240*(2), 318–332. https://doi.org/10.1148/radiol.2402050314.

Jernigan, T. L., Archibald, S. L., Fennema-Notestine, C., Taylor, M. J., Theilmann, R. J., Julaton, M. D., et al. (2011). Clinical factors related to brain structure in HIV: The CHARTER study. *Journal of Neurovirology, 17*(3), 248–257. https://doi.org/10.1007/s13365-011-0032-7.

Johnson, E. E., & Wessling-Resnick, M. (2012). Iron metabolism and the innate immune response to infection. *Microbes and Infection, 14*(3), 207–216. https://doi.org/10.1016/j.micinf.2011.10.001.

Kallianpur, A. R., & Levine, A. J. (2014). Host genetic factors predisposing to HIV-associated neurocognitive disorder. *Curr HIV/AIDS Reports, 11*(3), 336–352. https://doi.org/10.1007/s11904-014-0222-z.

Kallianpur, A. R., Jia, P., Ellis, R. J., Zhao, Z., Bloss, C., Wen, W., et al. (2014). Genetic variation in iron metabolism is associated with neuropathic pain and pain severity in HIV-infected patients on antiretroviral therapy. *PLoS One, 9*(8), e103123. https://doi.org/10.1371/journal.pone.0103123.

Kuhn, L. C. (2015). Iron regulatory proteins and their role in controlling iron metabolism. *Metallomics, 7*(2), 232–243. https://doi.org/10.1039/c4mt00164h.

Levine, A. J., Panos, S. E., & Horvath, S. (2014). Genetic, transcriptomic, and epigenetic studies of HIV-associated neurocognitive disorder. *Journal of Acquired Immune Deficiency Syndromes, 65*(4), 481–503. https://doi.org/10.1097/QAI.0000000000000069.

Li, X., Yang, Y., Zhou, F., Zhang, Y., Lu, H., Jin, Q., et al. (2011). SLC11A1 (NRAMP1) polymorphisms and tuberculosis susceptibility: Updated systematic review and meta-analysis. *PLoS One, 6*(1), e15831. https://doi.org/10.1371/journal.pone.0015831.

Lushchak, O. V., Piroddi, M., Galli, F., & Lushchak, V. I. (2014). Aconitase post-translational modification as a key in linkage between Krebs cycle, iron homeostasis, redox signaling, and metabolism of reactive oxygen species. *Redox Report, 19*(1), 8–15. https://doi.org/10.1179/1351000213Y.0000000073.

Mangialasche, F., Baglioni, M., Cecchetti, R., Kivipelto, M., Ruggiero, C., Piobbico, D., et al. (2015). Lymphocytic mitochondrial aconitase activity is reduced in Alzheimer's disease and mild cognitive impairment. *Journal of Alzheimer's disease : JAD, 44*(2), 649–660. https://doi.org/10.3233/JAD-142052.

McDermid, J. M., van der Loeff, M. F., Jaye, A., Hennig, B. J., Bates, C., Todd, J., et al. (2009). Mortality in HIV infection is independently predicted by host iron status and SLC11A1 and HP genotypes, with new evidence of a gene-nutrient interaction. *The American Journal of Clinical Nutrition, 90*(1), 225–233. https://doi.org/10.3945/ajcn.2009.27709.

Miszkiel, K. A., Paley, M. N., Wilkinson, I. D., Hall-Craggs, M. A., Ordidge, R., Kendall, B. E., et al. (1997). The measurement of R2, R2* and R2' in HIV-infected patients using the prime sequence as a measure of brain iron deposition. *Magnetic Resonance Imaging, 15*(10), 1113–1119.

Nir, T. M., Jahanshad, N., Busovaca, E., Wendelken, L., Nicolas, K., Thompson, P. M., & Valcour, V. G. (2014). Mapping white matter integrity in elderly people with HIV. *Human Brain Mapping, 35*(3), 975–992. https://doi.org/10.1002/hbm.22228.

Panos, S. E., Hinkin, C. H., Singer, E. J., Thames, A. D., Patel, S. M., Sinsheimer, J. S., et al. (2013). Apolipoprotein-E genotype and human immunodeficiency virus-associated neurocognitive disorder: The modulating effects of older age and disease severity. *Neurobehav HIV Med, 5*, 11–22. https://doi.org/10.2147/NBHIV.S39573.

Patton, S. M., Wang, Q., Hulgan, T., Connor, J. R., Jia, P., Zhao, Z., et al. (2017). Cerebrospinal fluid (CSF) biomarkers of iron status are associated with CSF viral load, antiretroviral therapy, and demographic factors in HIV-infected adults. *Fluids Barriers CNS, 14*(1), 11. https://doi.org/10.1186/s12987-017-0058-1.

Pichler, I., Del Greco, M. F., Gogele, M., Lill, C. M., Bertram, L., Do, C. B., et al. (2013). Serum iron levels and the risk of Parkinson disease: A Mendelian randomization study. *PLoS Medicine, 10*(6), e1001462. https://doi.org/10.1371/journal.pmed.1001462.

Provencher, S. W. (2001). Automatic quantitation of localized in vivo 1H spectra with LCModel. *NMR in Biomedicine, 14*(4), 260–264.

Pugliese, A., Gennero, L., Pescarmona, G. P., Beccattini, M., Morra, E., Orofino, G., et al. (2002). Serum citrate levels, haptoglobin haplotypes and transferrin receptor (CD71) in patients with HIV-1 infection. *Infection, 30*(2), 86–89.

Puig, S., Ramos-Alonso, L., Romero, A. M., & Martinez-Pastor, M. T. (2017). The elemental role of iron in DNA synthesis and repair. *Metallomics, 9*(11), 1483–1500. https://doi.org/10.1039/c7mt00116a.

Saloner, R., Heaton, R. K., Campbell, L. M., Chen, A., Franklin, D. R. J., Ellis, R. J., et al. (2019). Effects of comorbidity burden and age on brain integrity in HIV. *AIDS, 33*(7), 1175–1185.

Sheppard, D. P., Iudicello, J. E., Bondi, M. W., Doyle, K. L., Morgan, E. E., Massman, P. J., et al. (2015). Elevated rates of mild cognitive impairment in HIV disease. *Journal of Neurovirology, 21*(5), 576–584. https://doi.org/10.1007/s13365-015-0366-7.

Spector, S. A., Singh, K. K., Gupta, S., Cystique, L. A., Jin, H., Letendre, S., et al. (2010). APOE epsilon4 and MBL-2 O/O genotypes are associated with neurocognitive impairment in HIV-infected plasma donors. *AIDS, 24*(10), 1471–1479. https://doi.org/10.1097/QAD.0b013e328339e25c.

Valcour, V., Chalermchai, T., Sailasuta, N., Marovich, M., Lerdlum, S., Suttichom, D., et al. (2012). Central nervous system viral invasion and inflammation during acute HIV infection. *The Journal of Infectious Diseases, 206*(2), 275–282. https://doi.org/10.1093/infdis/jis326.

Wendelken, L. A., Jahanshad, N., Rosen, H. J., Busovaca, E., Allen, I., Coppola, G., et al. (2016). ApoE epsilon4 is associated with cognition, brain integrity, and atrophy in HIV over age 60. *Journal of Acquired Immune Deficiency Syndromes, 73*(4), 426–432. https://doi.org/10.1097/QAI.0000000000001091.

Wright, P. W., Pyakurel, A., Vaida, F. F., Price, R. W., Lee, E., Peterson, J., et al. (2016). Putamen volume and its clinical and neurological correlates in primary HIV infection. *AIDS, 30*(11), 1789–1794. https://doi.org/10.1097/QAD.0000000000001103.

Yndart, A., Kaushik, A., Agudelo, M., Raymond, A., Atluri, V. S., Saxena, S. K., et al. (2015). Investigation of Neuropathogenesis in HIV-1 clade B and C infection associated with IL-33 and ST2 regulation. *ACS Chemical Neuroscience, 6*(9), 1600–1612. https://doi.org/10.1021/acschemneuro.5b00156.

Young, A. C., Yiannoutsos, C. T., Hegde, M., Lee, E., Peterson, J., Walter, R., et al. (2014). Cerebral metabolite changes prior to and after antiretroviral therapy in primary HIV infection. *Neurology, 83*(18), 1592–1600. https://doi.org/10.1212/WNL.0000000000000932.